PERGAMON

International Journal of Solids and Structures 36 (1999) 697–709

INTERNATIONAL JOURNAL OF SOLIDS and STRUCTURES

Stress intensity factors around a cylindrical crack in an interfacial zone in composite materials

Shouetsu Itou*, Yasufumi Shima

Department of Mechanical Engineering, Kanagawa University, Yokohama 221, Japan

Received 7 April 1997; in revised form 27 January 1998

Abstract

Axisymmetric stresses around a cylindrical crack in an interfacial cylindrical layer between an infinite elastic medium with a cylindrical cavity and a circular elastic cylinder made of another material have been determined. The material constants of the layer vary continuously from those of the infinite medium to those of the cylinder. Tension surrounding the cylinder and perpendicular to the axis of the cylinder is applied to the composite materials. To solve this problem, the interfacial layer is divided into several layers with different material properties. The boundary conditions are reduced to dual integral equations. The differences in the crack faces are expanded in a series so as to satisfy the conditions outside the crack. The unknown coefficients in the series are solved using the conditions inside the crack. Numerical calculations are performed for several thicknesses of the interfacial layer. Using these numerical results, the stress intensity factors are evaluated for infinitesimal thickness of the layer. © 1998 Elsevier Science Ltd. All rights reserved.

1. Introduction

Fiber reinforced composite materials are lightweight and strong and will rapidly replace conventional materials such as steel, aluminum and epoxy in aeronautics, high speed train transportation and the automotive industry. However, the interfacial zone between the fiber and the matrix in the materials is relatively weak and is inclined to fracture. Therefore, the problem of stress intensity factors around a cylindrical crack that appears in the zone or in the cylindrical thin layer must be solved.

Delale and Erdogan (1988) considered that the elastic constants vary continuously across the interfacial layer and they solved the two-dimensional problem for a crack in an interfacial nonhomogeneous layer between two dissimilar elastic half-planes. Recently, axisymmetric solutions have been determined for a penny-shaped crack in an interfacial nonhomogeneous layer between two dissimilar elastic half-spaces by Ozturk and Erdogan (1995, 1996).

* Corresponding author. Fax: 81454917915; e-mail: itouie@cc.kanagawa-u.ac.jp

0020–7683/99/$ - see front matter © 1998 Elsevier Science Ltd. All rights reserved
PII: S0020–7683(98)00041–9

As mentioned above, solutions for a cylindrical interfacial crack are useful in the fracture mechanics of fiber reinforced composite materials. Quite recently, Xue-Li and Duo (1996) provided the stresses around a cylindrical crack in a nonhomogeneous layer between an infinite elastic medium and a circular elastic cylinder embedded in it. They studied the problem under Mode III torsional loading. To our knowledge, the corresponding solution for Mode I loading has not been examined.

In the present paper, axisymmetric stresses are obtained for a cylindrical crack in the interfacial layer between circular elastic cylinder and an infinite elastic medium under tension surrounding the cylinder. It is assumed that the material constants vary continuously from those of the cylinder to those of the infinite medium. To solve the problem, the interfacial cylindrical layer is divided into several layers with different elastic constants. Application of the Fourier transformation technique reduces the boundary conditions to two dual integral equations. One of the equations is satisfied by expanding the differences of displacements in a series of functions which are zero outside the crack. Using the remaining boundary conditions inside the crack, the unknown coefficients in each series are determined.

If the number of the divided cylindrical layers increases, the stresses obtained are identical with those of the interfacial layer, of which the material constants vary continuously.

The stress intensity factors are computed numerically for several thicknesses of the layer. Using these results, the values of the stress intensity factors for a very thin layer are evaluated.

2. Fundamental equations

Let (r, θ, z) be a cylindrical coordinate system. As shown in Fig. 1, a circular cylinder (B) with radius r_b is fixed inside an infinite elastic body (C) containing a cylindrical cavity with radius r_c. An interfacial cylindrical layer (A) is denoted by $r_b \leqq r \leqq r_c$. The thickness of the layer is described by $h\ (= r_c - r_b)$. Young's modulus and Poisson's ratio of the cylinder (B), the interfacial layer (A) and the infinite body (C) are shown by (E_B, v_B), (E_A, v_A) and (E_C, v_C), respectively.

An interfacial crack is placed along the z-axis from $-a$ to $+a$ on $r = r_a$. For convenience, the interfacial layer (A) is further divided into the layer (A-1) denoted by $(r_b \leqq r \leqq r_a)$ and the layer

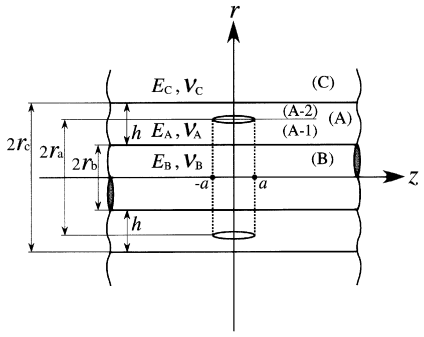

Fig. 1. Geometry and coordinate system.

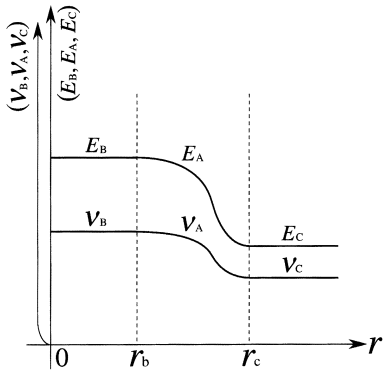

Fig. 2. Young's modulus and Poisson's ratio as a function of r.

(A-2) denoted by ($r_a \leqq r \leqq r_c$). Elastic constants (E_A, ν_A) most likely vary continuously in the interfacial layer with respect to r as shown in Fig. 2.

The stress and displacement components for an axisymmetric problem can be expressed by the equations:

$$\tau_{rr} = \partial/\partial z\{\nu\nabla^2 - \partial^2/\partial r^2\}\phi$$
$$\tau_{zz} = \partial/\partial z\{(2-\nu)\nabla^2 - \partial^2/\partial z^2\}\phi$$
$$\tau_{\theta\theta} = \partial/\partial z\{\nu\nabla^2 - (1/r)\partial/\partial r\}\phi$$
$$\tau_{rz} = \partial/\partial r\{(1-\nu)\nabla^2 - \partial^2/\partial z^2\}\phi \tag{1}$$
$$u_r = -(1+\nu)/E\,\partial^2\phi/\partial r\,\partial z$$
$$u_z = (1+\nu)/E\{(1-2\nu)\nabla^2 + \partial^2/\partial r^2 + (1/r)\,\partial/\partial r\}\phi \tag{2}$$

where ϕ is a biharmonic function which satisfies

$$\nabla^4\phi = 0 \tag{3}$$

with

$$\nabla^2 = \partial^2/\partial r^2 + (1/r)\,\partial/\partial r + \partial^2/\partial z^2. \tag{4}$$

The tension p, surrounding the cylinder and perpendicular to the z-axis, is assumed to be applied to the composite materials. Then, the stress intensity factors can be provided by solving the problem using the following boundary conditions:

$$\tau_{rrC} = \tau_{rrA2}, \quad \tau_{rzC} = \tau_{rzA2}, \quad u_{rc} = u_{rA2}, \quad u_{zC} = u_{zA2} \quad at\ r = r_c, \quad |z| < \infty \tag{5}$$
$$\tau_{rrA1} = \tau_{rrB}, \quad \tau_{rzA1} = \tau_{rzB}, \quad u_{rA1} = u_{rB}, \quad u_{zA1} = u_{zB} \quad at\ r = r_b, \quad |z| < \infty \tag{6}$$
$$\tau_{rrA1} = \tau_{rrA2}, \quad \tau_{rzA1} = \tau_{rzA2} \quad \text{at } r = r_a, \quad |z| < \infty \tag{7}$$
$$\tau_{rrA1} = -p, \quad \tau_{rzA1} = 0 \quad \text{at } r = r_a, \quad 0 \leqq |z| < a \tag{8}$$

$$u_{rA1} = u_{rA2}, \quad u_{zA1} = u_{zA2} \quad \text{at } r = r_a, \quad a < |z| < \infty \tag{9}$$

where p is a constant and the variables with subscripts $A1$, $A2$, B, C are those for layers (A-1), (A-2), cylinder (B) and infinite body (C), respectively.

3. Division of interfacial layer

The interfacial cylindrical layer (A) in Fig. 1 is divided into several layers, where the number, m, of the divided layers must be odd. To illustrate the process of solving the problem, m is set to three. Namely, the interfacial layer (A) is divided into layer (1) occupying $r_b \leqq r \leqq r_1$, layer (2) occupying $r_1 \leqq r \leqq r_2$, and layer (3) occupying $r_2 \leqq r \leqq r_c$ as shown in Fig. 3. Layer (2) which contains the cylindrical crack is further divided into layer (2)-1 occupying $r_1 \leqq r \leqq r_a$ and layer (2)-2 occupying $r_a \leqq r \leqq r_2$.

Here, the material constants in the interfacial layer (A) are assumed to vary linearly with respect to r. Then, E_A and v_A are expressed by

$$\begin{aligned} E_A &= (E_c - E_B)/(r_c - r_b) \times (r - r_b) + E_B \\ v_A &= (v_c - v_B)/(r_c - r_b) \times (r - r_b) + v_B. \end{aligned} \tag{10}$$

For $m = 3$, the material constants of layers (1), (2), (3) take the average values (E_1, v_1), (E_2, v_2), (E_3, v_3) instead of (E_A, v_A) as seen in Fig. 4.

Then, the boundary conditions (5)–(9) can be expressed by the following equations:

$$\tau_{rrC} = \tau_{rr3}, \quad \tau_{rzC} = \tau_{rz3}, \quad u_{rc} = u_{r3}, \quad u_{zC} = u_{z3} \quad at\ r = r_c, \quad |z| < \infty \tag{11}$$

$$\tau_{rr3} = \tau_{rr22}, \quad \tau_{rz3} = \tau_{rz22}, \quad u_{r3} = u_{r22}, \quad u_{z3} = u_{z22} \quad at\ r = r_2, \quad |z| < \infty \tag{12}$$

$$\tau_{rr21} = \tau_{rr1}, \quad \tau_{rz21} = \tau_{rz1}, \quad u_{r21} = u_{r1}, \quad u_{z21} = u_{z1} \quad at\ r = r_1, \quad |z| < \infty \tag{13}$$

$$\tau_{rr1} = \tau_{rrB}, \quad \tau_{rz1} = \tau_{rzB}, \quad u_{r1} = u_{rB}, \quad u_{z1} = u_{zB} \quad at\ r = r_b, \quad |z| < \infty \tag{14}$$

$$\tau_{rr22} = \tau_{rr21}, \quad \tau_{rz22} = \tau_{rz21}, \quad \text{at } r = r_a, \quad |z| < \infty \tag{15}$$

$$\tau_{rr22} = -p, \quad \tau_{rz22} = 0 \quad \text{at } r = r_a, \quad 0 \leqq |z| < a \tag{16}$$

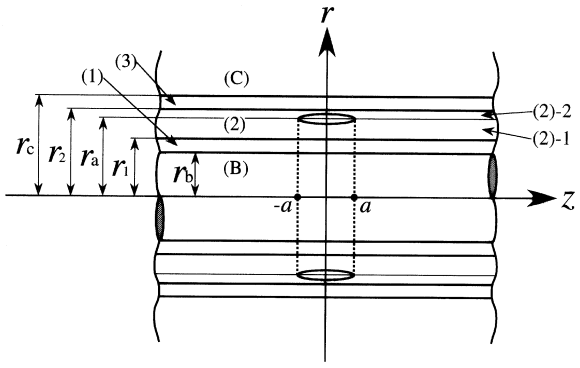

Fig. 3. Interfacial layer replaced by three layers.

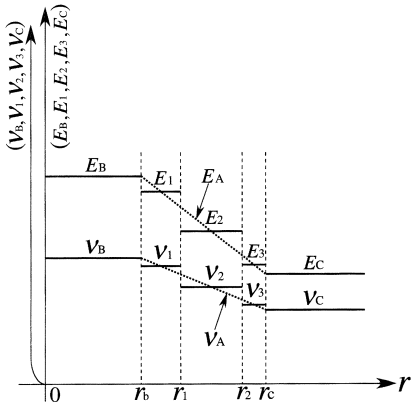

Fig. 4. Material constants in replaced layers.

$$u_{r22} = u_{r21}, \quad u_{z22} = u_{z21} \quad \text{at } r = r_a, \quad a < |z| < \infty \tag{17}$$

where the variables with subscripts 1, 21, 22, 3 are those for layers (1), (2)-1, (2)-2 and (3), respectively.

4. Analysis

To find the solution of eqn (3), the Fourier transforms which are defined by

$$\bar{f}(\xi) = \int_{-\infty}^{\infty} f(z) \exp(i\xi z)\, \mathrm{d}z, \quad f(z) = 1/(2\pi) \int_{-\infty}^{\infty} \bar{f}(\xi) \exp(-i\xi z)\, \mathrm{d}\xi \tag{18}$$

are introduced. Applying eqn (18) to eqn (3) yields

$$(\partial^2/\partial r^2 + 1/r \times \partial/\partial r - \xi^2)^2 \bar{\phi} = 0. \tag{19}$$

The solutions of eqn (19) have the following forms for the layers (i) ($i = 1, 21, 22, 3$):

$$\bar{\phi}_i = A_{1i}(\xi) K_0(\xi r) + A_{2i}(\xi) \xi r K_1(\xi r) + B_{1i}(\xi) I_0(\xi r) + B_{2i}(\xi) \xi r I_1(\xi r). \tag{20}$$

For the cylinder (B) and the infinite body (C), $\bar{\phi}_i$ are given by

$$\bar{\phi}_B = B_{1B}(\xi) I_0(\xi r) + B_{2B}(\xi) \xi r I_1(\xi r)$$
$$\bar{\phi}_C = A_{1C}(\xi) K_0(\xi r) + A_{2C}(\xi) \xi r K_1(\xi r). \tag{21}$$

In eqns (20) and (21), $I_n(\xi r)$ and $K_n(\xi r)$ are modified Besel functions of the first and second kind, respectively, and $A_{1i}(\xi)$, $A_{2i}(\xi)$, ..., $A_{2C}(\xi)$ are unknown coefficients. By substituting eqns (20) and (21) into eqns (1) and (2) in the Fourier transform domain, Fourier transformed expressions of stresses and displacements are obtained. Then, the boundary conditions (11), (12), (13), (14) and (15), which are valid for $|z| < \infty$, can be easily satisfied.

To satisfy the boundary condition (17), differences $(u_{r22} - u_{r21})$ and $(u_{z22} - u_{z21})$ at $r = r_a$ are represented in the series expansions

$$(u_{r22}-u_{r21}) = \sum_{n=1}^{\infty} c_n \cos\{(2n-1)\sin^{-1}(z/a)\} \quad \text{for } |z| < a$$

$$= 0 \quad \text{for } a < |z| \tag{22}$$

$$(u_{z22}-u_{z21}) = \sum_{n=1}^{\infty} d_n \sin\{2n\sin^{-1}(z/a)\} \quad \text{for } |z| < a$$

$$= 0 \quad \text{for } a < |z| \tag{23}$$

where c_n and d_n are unknown coefficients that need to be determined. Then, it is easily shown that stresses that satisfy the boundary conditions (11)–(15) and (17) can be expressed by the unknown coefficients c_n and d_n. For example, stresses τ_{rr22} and τ_{rz22} at $r = r_a$ are given by

$$\tau_{rr22} = \sum_{n=1}^{\infty} c_n(2n-1)/\pi \int_0^{\infty} Q_1(\xi)/\xi J_{2n-1}(a\xi)\cos(\xi z)\mathrm{d}\xi$$

$$+ \sum_{n=1}^{\infty} d_n(2n)/\pi \int_0^{\infty} Q_2(\xi)/\xi J_{2n}(a\xi)\cos(\xi z)\,\mathrm{d}\xi$$

$$\tau_{rz22} = \sum_{n=1}^{\infty} c_n(2n-1)/\pi \int_0^{\infty} Q_3(\xi)/\xi J_{2n-1}(a\xi)\sin(\xi z)\,\mathrm{d}\xi$$

$$+ \sum_{n=1}^{\infty} d_n(2n)/\pi \int_0^{\infty} Q_4(\xi)/\xi J_{2n}(a\xi)\sin(\xi z)\,\mathrm{d}\xi \tag{24}$$

where $J_n(\xi)$ is the Bessel function and the expressions of known functions $Q_1(\xi)$, $Q_2(\xi)$, $Q_3(\xi)$, $Q_4(\xi)$ are complex and have been omitted. The semi-infinite integrals in eqn (24) must be evaluated by numerical integration. If functions $Q_1(\xi)$, $Q_2(\xi)$, $Q_3(\xi)$, $Q_4(\xi)$ are calculated numerically, the results will show that $Q_2(\xi)$ is equal to $Q_3(\xi)$ and decaies rapidly as ξ increases. Functions $Q_i(\xi)$ ($i = 1$ and 4) are proportional to ξ as ξ increases, namely

$$Q_i(\xi)/\xi \to Q_i^L, \quad \text{for } i = 1 \quad \text{and} \quad 4. \tag{25}$$

In eqn (25), constants Q_i^L can be calculated by

$$Q_i^L = Q_i(\xi_L)/\xi_L \tag{26}$$

with ξ_L being a large value of ξ.

Finally, the remaining boundary condition (16) can be reduced to the equations

$$\sum_{n=1}^{\infty} c_n g_n(z) + \sum_{n=1}^{\infty} d_n h_n(z) = -p$$

$$\sum_{n=1}^{\infty} c_n k_n(z) + \sum_{n=1}^{\infty} d_n l_n(z) = 0 \quad \text{for } 0 \leqq z < a \tag{27}$$

with

$$g_n(z) = (2n-1)/\pi\left[\int_0^\infty \{Q_1(\xi)/\xi - Q_1^L\}J_{2n-1}(a\xi)\cos(\xi z)\,\mathrm{d}\xi + Q_1^L \cos\{(2n-1)\sin^{-1}(z/a)\}/(a^2-z^2)^{1/2}\right]$$

$$h_n(z) = 2n/\pi\int_0^\infty Q_2(\xi)/\xi J_{2n}(a\xi)\cos(\xi z)\,\mathrm{d}\xi$$

$$k_n(z) = (2n-1)/\pi\int_0^\infty Q_3(\xi)/\xi J_{2n-1}(a\xi)\sin(\xi z)\,\mathrm{d}\xi$$

$$l_n(z) = 2n/\pi\left[\int_0^\infty \{Q_4(\xi)/\xi - Q_4^L\}J_{2n}(a\xi)\sin(\xi z)\,\mathrm{d}\xi + Q_4^L \sin\{2n\sin^{-1}(z/a)\}/(a^2-z^2)^{1/2}\right]. \quad (28)$$

The integrands in eqn (28) decrease rapidly and thus numerical integrations can be performed. Equation (27) can be solved for coefficients c_n and d_n using the Schmidt method (Yau, 1967).

Stresses at $r = r_a$ are given by eqn (24). Using the relations

$$\int_0^\infty J_n(a\xi)\{\cos(\xi z), \sin(\xi z)\}\,\mathrm{d}\xi = [-a^n(z^2-a^2)^{-1/2}\{z+(z^2-a^2)^{1/2}\}^{-n}\sin(n\pi), \; a^n(z^2-a^2)^{-1/2}\{z+(z^2-a^2)^{1/2}\}^{-n}\cos(n\pi)] \quad (29)$$

the stress intensity factors can be defined by

$$K_1 = \{2\pi(z-a)\}^{1/2}\tau_{rr22}|_{z\to a+} = \sum_{n=1}^{\infty} c_n Q_1^L(2n-1)(-1)^n/(\pi a)^{1/2}$$

$$K_2 = \{2\pi(z-a)\}^{1/2}\tau_{rz22}|_{z\to a+} = \sum_{n=1}^{\infty} d_n Q_4^L(2n)(-1)^n/(\pi a)^{1/2}. \quad (30)$$

In Sections 3 and 4, stress intensity factors were solved only for $m = 3$. It is quite straightforward to obtain the solutions for $m = 1, 5, 7$. The values K_1 and K_2 are calculated numerically for $m = 1$, 3, 5, 7 and are plotted vs $1/m$. Then, the results for the interfacial layer, of which the material constants vary continuously with respect to r, can be obtained by the values for $1/m \to 0$. This process is explained in detail below.

5. Numerical results

Numerical calculations are carried out for $r_a = r_b + h/2$ ($= r_c - h/2$). Namely, the cylindrical crack is situated on the middle-surface of the interfacial cylindrical layer. It is assumed that

Table 1
Values of $Q_i(\xi a)/(\xi a)$ $(i = 1, 2, 3, 4)$ for $r_a/a = 1.0$, $h/(2a) = 0.05$, $E_B/E_C = 10.0$ and $m = 7$

(ξa)	$Q_1(\xi a)/(\xi a)$	$Q_2(\xi a)/(\xi a)$	$Q_3(\xi a)/(\xi a)$	$Q_4(\xi a)/(\xi a)$
0.01	-0.8626539×10^{2}	-0.2594474×10^{0}	-0.25594474×10^{0}	-0.4938311×10^{-1}
0.21	-0.4268333×10^{1}	-0.2959433×10^{0}	-0.2959433×10^{0}	-0.5828979×10^{0}
237.81	-0.1496055×10^{1}	-0.5437340×10^{-1}	-0.5437340×10^{-1}	-0.1507008×10^{1}
238.01	-0.1496085×10^{1}	-0.5430096×10^{-1}	-0.5430096×10^{-1}	-0.1507011×10^{1}
475.81	-0.1509661×10^{1}	-0.7089578×10^{-2}	-0.7089578×10^{-2}	-0.1510247×10^{1}
476.01	-0.1509664×10^{1}	-0.7075708×10^{-2}	-0.7075708×10^{-2}	-0.1510248×10^{1}

Table 2
Values for the left hand side of eqn (27) for $r_a/a = 1.0$, $h/(2a) = 0.05$, $E_B/E_C = 10.0$ and $m = 7$

	$\sum_{n=1}^{18}\{c_n g_n(z/a)+d_n h_n(z/a)\}/p$	$\sum_{n=1}^{18}\{c_n k_n(z/a)+d_n l_n(z/a)\}/p$
$z/a = 0.00100$	1.000004	0.000001
0.02632	1.000000	0.000000
0.50000	1.000000	0.000000
0.97368	1.000000	0.000000
0.99900	1.000000	0.000000

Poisson's ratio v_B is equal to v_C, and that they have a value of 0.3. Equation (10) shows that $v_A = 0.3$. The interfacial layer (A) is divided into m layers with the same thickness, h/m.

Functions $g_n(z)$, $h_n(z)$, $k_n(z)$ and $l_n(z)$ contain an infinite integral. The integrands in these functions decay rapidly as the integration variable ξ increases. The functions themselves decrease more slowly according to the decreases in both the h/a and E_C/E_B ratios. In Table 1, the values of $Q_i(\xi a)/(\xi a)$ $(i = 1, 2, 3, 4)$ are denoted for $r_a/a = 1.0$, $h/(2a) = 0.05$, $E_B/E_C = 10.0$ and $m = 7$. As indicated in the table, numerical integrations can be satisfactorily performed. The accuracy of the Schmidt method decreases as both the h/a and E_C/E_B ratios decrease. To solve c_n and d_n in eqn (27), the Schmidt method has been applied by truncating the infinite series in eqn (27) at N. In Table 2, the values for the left hand side of eqn (27) are shown for $r_a/a = 1.0$, $h/(2a) = 0.05$, $E_B/E_C = 10.0$ and $m = 7$, where N is set at 18. From the Table, it can be seen that the Schmidt method has been applied satisfactorily. In order to verify whether the result of the stress intensity factor converges to a constant value as N increases, the stress intensity factors K_1 and K_2 are plotted vs N in Fig. 5. Clearly convergence is excellent.

As mentioned above, the infinite integrals contained in $g_n(z)$, $h_n(z)$, $k_n(z)$ and $l_n(z)$ must be evaluated numerically. For $r_a/a = 1.0$, $h/(2a) = 0.05$, $E_B/E_C = 10.0$, $m = 7$ and $N = 18$, the infinite integrals are calculated taking the upper limit of integration as $(\xi_L a) = 50.01, 100.01, \ldots, 400.01$ and 476.01. In Fig. 6, the stress intensity factors K_1 and K_2 are shown with respect to $(\xi_L a)$. From

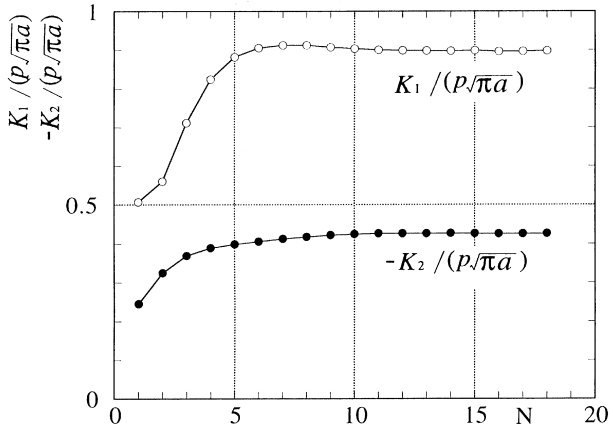

Fig. 5. Stress intensity factors K_1 and K_2 for $r_a/a = 1.0$, $h/(2a) = 0.05$, $E_B/E_C = 10.0$, $m = 7$ vs N.

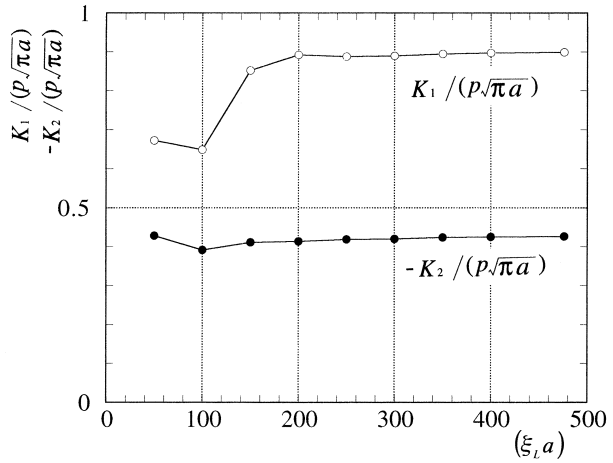

Fig. 6. Stress intensity factors K_1 and K_2 for $r_a/a = 1.0$, $h/(2a) = 0.05$, $E_B/E_C = 10.0$, $m = 7$, $N = 18$ vs $(\xi_L a)$.

this, it is clear that the stress intensity factors converge to constant values when the upper limit of integration in the infinite integrals is replaced by a larger value.

Next, the stress intensity factors K_1 and K_2 are calculated for $r_a/a = 1.0$, $h/(2a) = 0.05$, $E_B/E_C = 10.0$ and $m = 1, 3, 5, 7$. The results of the stress intensity factors K_1 and K_2, which are plotted vs $1/m$ in Fig. 7, lie in straight lines. The material constants are thought to vary continuously across the actual interfacial layer. However, the values of the stress intensity factors for the layer can be given if the interfacial layer is replaced by the divided layers of the infinite number. Namely, the values can be provided by those at $1/m \to 0$ in Fig. 7.

The interfacial cylindrical layer between the fiber and the matrix is very thin. However, as the value of the thickness h decreases or as the E_C/E_B ratio decreases, more and more terms are required to solve coefficients c_n and d_n using the Schmidt method. When the infinite series in eqn (27) is

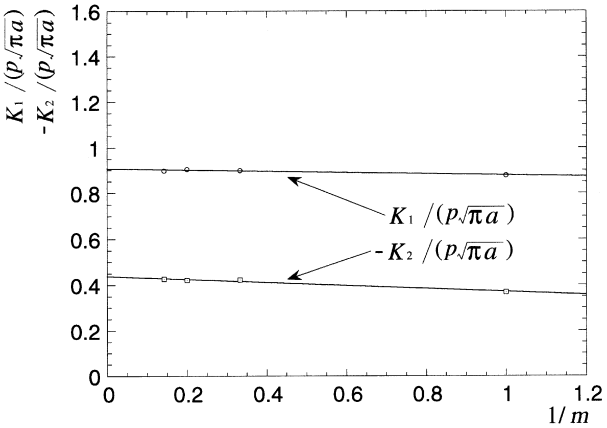

Fig. 7. Stress intensity factors K_1 and K_2 for $r_a/a = 1.0$, $h/(2a) = 0.05$, $E_B/E_C = 10.0$ vs $1/m$.

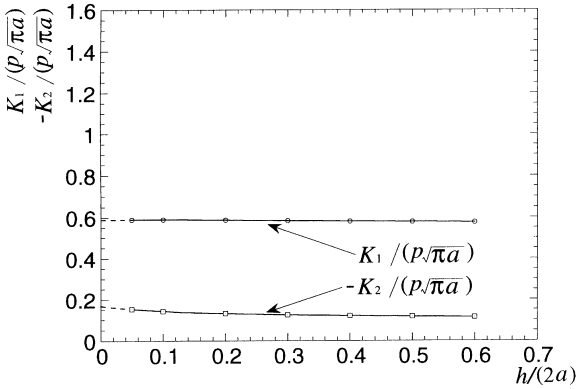

Fig. 8. Stress intensity factors K_1 and K_2 for $r_a/a = 1.0$, $E_B/E_C = 2.0$.

truncated by a value larger than $n = 18$, overflows occur in the process of numerical calculations. Therefore, the stress intensity factors K_1 and K_2 cannot be provided for $h/(2a) < 0.05$.

In Figs 8–11, the stress intensity factors K_1 and K_2 are plotted vs $h/(2a)$ for $r_a/a = 1.0$ and $E_B/E_C = 2.0, 4.0, 8.0, 10.0$. In these figures, the values for $h/(2a) < 0.05$ are not calculated numerically and the broken lines for the range are given by curves of the fourth degree, which are determined using the calculated values of $h/(2a) = 0.05, 0.1, 0.2, 0.3, 0.4$. The curves of K_1 and K_2 vs $1-(E_C/E_B)$ are shown in Figs 12 and 13, respectively, where the broken lines are plotted using the values for $h/(2a) \to 0$ in Figs 8–11. The values for $\{1-(E_C/E_B)\} = 0.0$ are identical with those calculated for a cylindrical crack in an homogeneous isotropic solid (Kasano et al., 1984).

6. Discussion

In the present paper, stress intensity factors are analysed under the assumption that the material constants in the interfacial layer vary linearly with respect to r. For any variations of the material

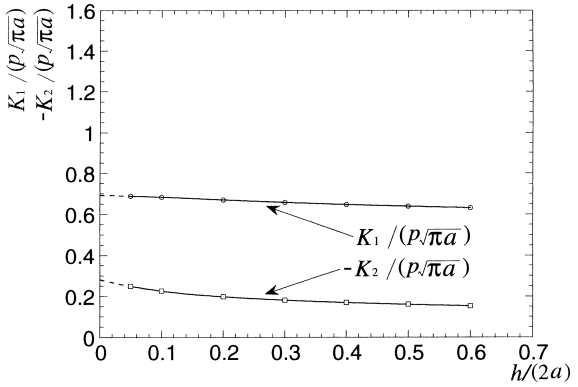

Fig. 9. Stress intensity factors K_1 and K_2 for $r_a/a = 1.0$, $E_B/E_C = 4.0$.

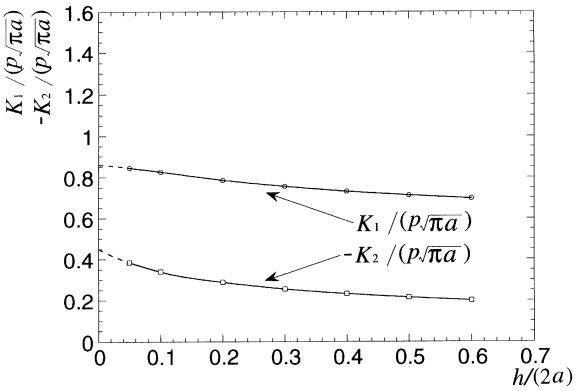

Fig. 10. Stress intensity factors K_1 and K_2 for $r_a/a = 1.0$, $E_B/E_C = 8.0$.

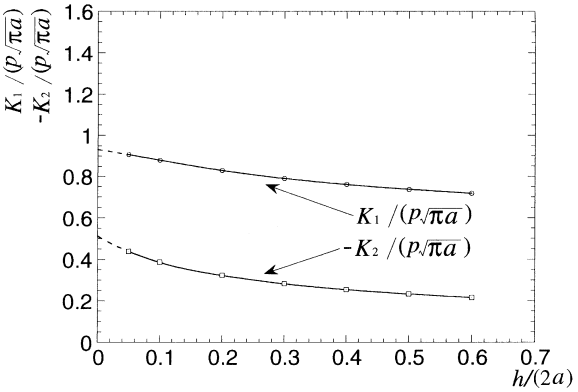

Fig. 11. Stress intensity factors K_1 and K_2 for $r_a/a = 1.0$, $E_B/E_C = 10.0$.

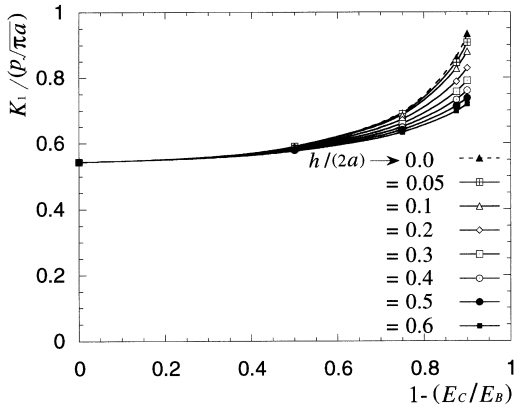

Fig. 12. Stress intensity factors K_1 for $r_a/a = 1.0$ vs $1-(E_C/E_B)$.

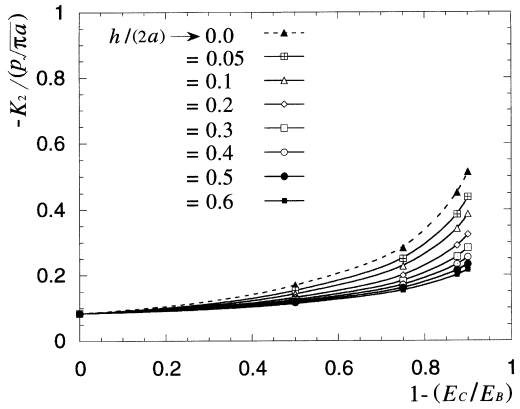

Fig. 13. Stress intensity factors K_2 for $r_a/a = 1.0$ vs $1-(E_C/E_B)$.

property in the interfacial layer, the stress intensity factors can be obtained in a straightforward manner. In numerical calculations, the cylindrical crack is assumed to be situated on the middle-surface of the interfacial cylindrical layer. In addition, there appears to be no difficulty in calculating the stress intensity factors around an arbitrarily situated crack.

Any interfacial zone that exists in fiber reinforced plastics is very thin. Thus, the actual values of the stress intensity factors around the cylindrical crack in the interfacial layer may be considered to be expressed by the broken curves in Figs 12 and 13. These values steadily increase as the E_C/E_B ratio decreases. Consequently, selection of reinforcement that has a Young's modulus not much larger than that of the matrix is advisable.

If the E_B/E_C ratio is smaller than 2.0, that is, the value $(1-E_C/E_B)$ is smaller than 0.5, the effect of the ratio on both K_1 and K_2 around a cylindrical crack in an interfacial zone is negligible.

References

Delale, F., Erdogan, F., 1988. On the mechanical modeling of the interfacial region in bonded half-planes. ASME J. Appl. Mech. 55, 317–324.

Kasano, H., Matsumoto, H., Nakahara, I., 1984. A torsion-free axisymmetric problem of a cylindrical crack in a transversely isotropic body. Bulletin of Japan Soc. Mech. Engrs 27, 1323–1332.

Ozturk, M., Erdogan, F., 1995. An axisymmetric crack in bonded materials with a nonhomogeneous interfacial zone. ASME J. Appl. Mech. 62, 116–125.

Ozturk, M., Erdogan, F., 1996. Axisymmetric crack problem in bonded materials with a graded interfacial region. Int. J. Solids and Structures 33, 193–219.

Xue-Li, H., Duo, W., 1996. The crack problem of a fiber-matrix composite with a nonhomogeneous interfacial zone under torsional loading—Part I. A cylindrical crack in the interfacial zone. Engng Fracture Mech. 54, 63–69.

Yau, W.F., 1967. Axisymmetric slipless indentation of an infinite elastic cylinder. SIAM J. Appl. Math. 15, 219–227.